Geol. Mag.: page 1 of 18 © *Cambridge University Press 2016*
doi:10.1017/S0016756816001023

Benthic foraminiferal response to relative sea-level changes in the Maastrichtian–Danian succession at the Dakhla Oasis, Western Desert, Egypt

SHERIF FAROUK*† & SREEPAT JAIN‡

*Exploration Department, Egyptian Petroleum Research Institute, Nasr City, 11727, Egypt
‡Department of Applied Geology, Adama Science and Technology University, School of Applied Natural Sciences, P.O. Box 1888, Adama, Ethiopia

(*Received* 13 June 2016; *accepted* 11 October 2016)

Abstract – The Maastrichtian–Danian benthic foraminiferal diversity and assemblages through sequence stratigraphy were studied at Dakhla Oasis, Egypt. Benthic foraminifera numbers (BFN), high-flux species and characteristic benthic foraminiferal species and genera distribution are also incorporated to assess palaeobathymetry, palaeoenvironment and palaeoproductivity. All these proxies are then taken together to construct a sea-level curve and interpreted in terms of regional tectonics, climate and eustasy. Data suggest a remarkably highly equitable benthic environment deposited in a brackish littoral and/or marsh setting with moderate (?) to low oxygen conditions and reduced salinity (oligotrophic), possibly due to increased precipitation and terrestrial runoff. The interrupted dominance of calcareous forms and high-organic-flux species suggests occasional marine incursions and high palaeoproductivity, due to local upwelling. The inferred sea-level curve replicates the global eustatic curve and suggests that the curve is more influenced by the prevailing climate and global eustasy rather than by regional tectonics. The post-Cretaceous–Palaeogene boundary displays improvement in the environment in terms of diversity and number of species and specimens, with a marked reduction in the abundance of high-organic-flux species during early Paleocene (Danian) time, indicating a shift from a more mesotrophic open marine environment to much reduced oligotrophic conditions.

Keywords: Foraminifera, sequence stratigraphy, Western Desert, Egypt, Maastrichtian.

1. Introduction

The Upper Cretaceous – lower Palaeogene stratigraphic succession exposed in the Western Desert has been the subject of intensive studies (Le Roy, 1953; Said & Kerdany, 1961; Hewaidy & Cherif, 1984; Luger, 1985, 1988; Anan & Hewaidy, 1986; Cherif & Hewaidy, 1986; Hewaidy, 1990; Samir, 1995; Schnack, 2000; Hewaidy & Strougo, 2001; Hewaidy *et al.* 2014; Orabi & Khalil, 2014; Farouk & El-Sorogy, 2015; El-Dawy *et al.* 2016). However, palaeoenvironment and palaeobathymetry studies using smaller benthic foraminifera have been scarce, especially in the Dakhla Oasis (Schnack, 2000; Hewaidy *et al.* 2014) (Fig. 1a, b).

In the present study, benthic foraminiferal species distribution (abundance patterns) are used to build assemblages and characteristic species, corroborate palaeoenvironmental data and infer palaeobathymetry (Luger, 1985, 1988; Hewaidy, 1990; Speijer, 1994; Speijer & Van Der Zwaan, 1996; Li, Keller & Stinnesbeck, 1999; El Deep, Faris & Mandur, 2000; Schnack, 2000; Tantawy *et al.* 2001; Keller *et al.* 2002; Jain & Collins, 2007; Jain, Collins & Hayek, 2007; Nagy *et al.* 2001, 2011; King, 2013).

Diversity measures (Shannon H, Fisher's α, equitability and dominance), benthic foraminifera number (BFN) and species abundances are used for first time in the Western Desert of Egypt better interpret the prevailing palaeoenvironment. These proxies have previously been used to infer benthic ecological structure and depositional environment (Smart, 1998; Murray 2006; Nagy, Hess & Alve, 2010; Nagy *et al.* 2011; Hess, Nagy & Laursen, 2014).

The response of benthic foraminiferal assemblages to relative sea-level changes during the Maastrichtian–Danian succession of the Dakhla Oasis (Egypt) is analysed with respect to sequence stratigraphy, regional tectonics, climate and sea-level changes. The pre- and post-Cretaceous–Palaeogene (K/Pg) distribution of high-organic-flux benthic foraminiferal species is also analysed to better understand the prevailing environment in terms of changes in nutrient availability.

2. Geological setting

The Dakhla Oasis is a large topographic depression located in the central Western Desert of Egypt, marked by a less deformed and stable tectonic shelf (Said, 1962) (Fig. 1). The Western Desert is generally characterized by submerged and varying palaeo-lows and highs (El-Azabi & Farouk, 2011; Farouk & El-Sorogy,

---

†Author for correspondence: geo.sherif@hotmail.com

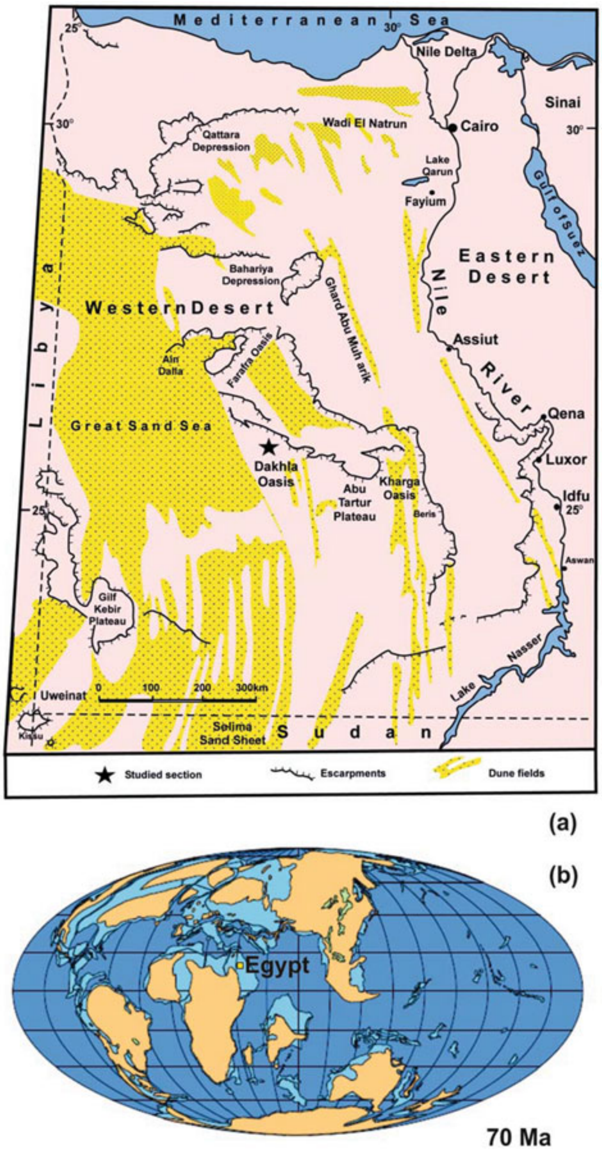

Figure 1. (Colour online) Study area: (a) location map showing the study area (star), southern Western Desert, Egypt and (b) palaeogeographic set-up of the study area, Egypt.

2015) (Fig. 2a). The stratigraphic succession in the Dakhla–Kharga oases is subdivided into the Upper Jurassic – lower–middle Campanian, lower siliciclastic (= the Nubian Sandstone) and the upper Campanian – lower Eocene siliciclastics/carbonate sequences (Fig. 2b), which are covered by Quaternary deposits.

Three lateral and vertical facies changes in the Western Desert of Egypt are well known from north to south as (1) Farafra Facies, including (from oldest to youngest): Campanian El–Hefhuf; Maastrichtian Khoman Chalk; Danian Dakhla Shale; Selandian–Thanetian Tarawan Chalk; Thanetian–Ypresian Esna Shale and its lateral equivalent the Ain Dalla; and Ypresian Farafra Limestone formations; (2) Nile Valley Facies including (from oldest to youngest): Campanian Duwi; Maastrichtian–Selandian Dakhla Shale; Thanetian Tarawan Chalk; Thanetian–Ypresian Esna Shale; and Ypresian Thebes Limestone formations; and (3) the Garra El–Arbian Facies including: Maastrichtian Dakhla Shale; Danian–Selandian Kurkur; and Thanetian Garra formations (Fig. 2a, b). The present study is related to the Nile Valley Facies and is restricted to the Maastrichtian–Danian Dakhla Shale Formation (Fig. 2). It is classified into three members: the Early Maastrichtian Mawhoob Shale; the Late Maastrichtian Beris Oyster Mudstone; and the Late Maastrichtian – Paleocene Kharga Shale Member (Awad & Ghobrial, 1965; Figs 2a–c, 3). The latter is further subdivided into two informal units, the Lower and Upper Kharga Shale Members (Luger, 1985), separated by the Cretaceous–Palaeogene (K/Pg) boundary (Figs 2, 3). The Maastrichtian Mawhoob Shale and Beris Oyster Mudstone members pass laterally towards the north at the Farafra Oasis into the Khoman Chalk Formation (Figs 2, 3).

3. Biostratigraphy

The studied sediments of the Dakhla Formation range from Maastrichtian to Danian in age (Fig. 4). The Maastrichtian interval is classified according to the biostratigraphic zonal schemes of Li, Keller & Stinnesbeck (1999) and the Paleocene interval according to Berggren & Pearson (2005). Five zones are recognized (Fig. 4), described in the following sections.

3.a. *Rugoglobigerina hexacamerata* Zone (CF8b)

This zone is defined by the LO of *Rugoglobigerina hexacamerata* Brönnimann to the LO of *Gansserina gansseri* (Bolli). It is equivalent to the lowermost part of the Mawhoob Shale Member (samples 1–7, Fig. 4) which overlies the barren late Campanian sediments of the Duwi Formation. The dominant planktonic foraminiferal species recorded in this zone include *Globotruncana arca* (Cushman), *G. aegyptiaca* Nakkady, *G. orientalis* El-Naggar, *Globotruncanita stuartiformis* (Dalbiez), *G. stuarti* (de Lapparent), *Contusotruncana fornicata* (Plummer), *Rugoglobigerina rugosa* (Plummer), *R. macrocephala* Brönnimann, *Heterohelix globulosa* (Ehrenberg), *H. navaroensis* Loeblich, *H. reussi* (Cushman) and *H. striata* (Ehrenberg).

3.b. *Gansserina gansseri* Zone (CF7)

This is defined as the biostratigraphic interval from the first appearance of *Gansserina gansseri* (Bolli) to the first appearance of *Contusotruncana contusa* (Cushman) of early Maastrichtian age (samples 8–17, Fig. 4) of the Mawhoob Shale Member. The planktonic foraminiferal assemblage is similar to that of the underlying CF8b Zone, with the addition of the nominate taxon (G. gansseri) and *Pseudoguembelina palpebra* Brönnimann and Brown. Farouk (2014) had earlier noted that the first occurrence (FO) of the *G. gansseri* event is relatively stratigraphically high in the Middle East (Tunisia, Jordan and Egypt) within the middle part of early Maastrichtian age.

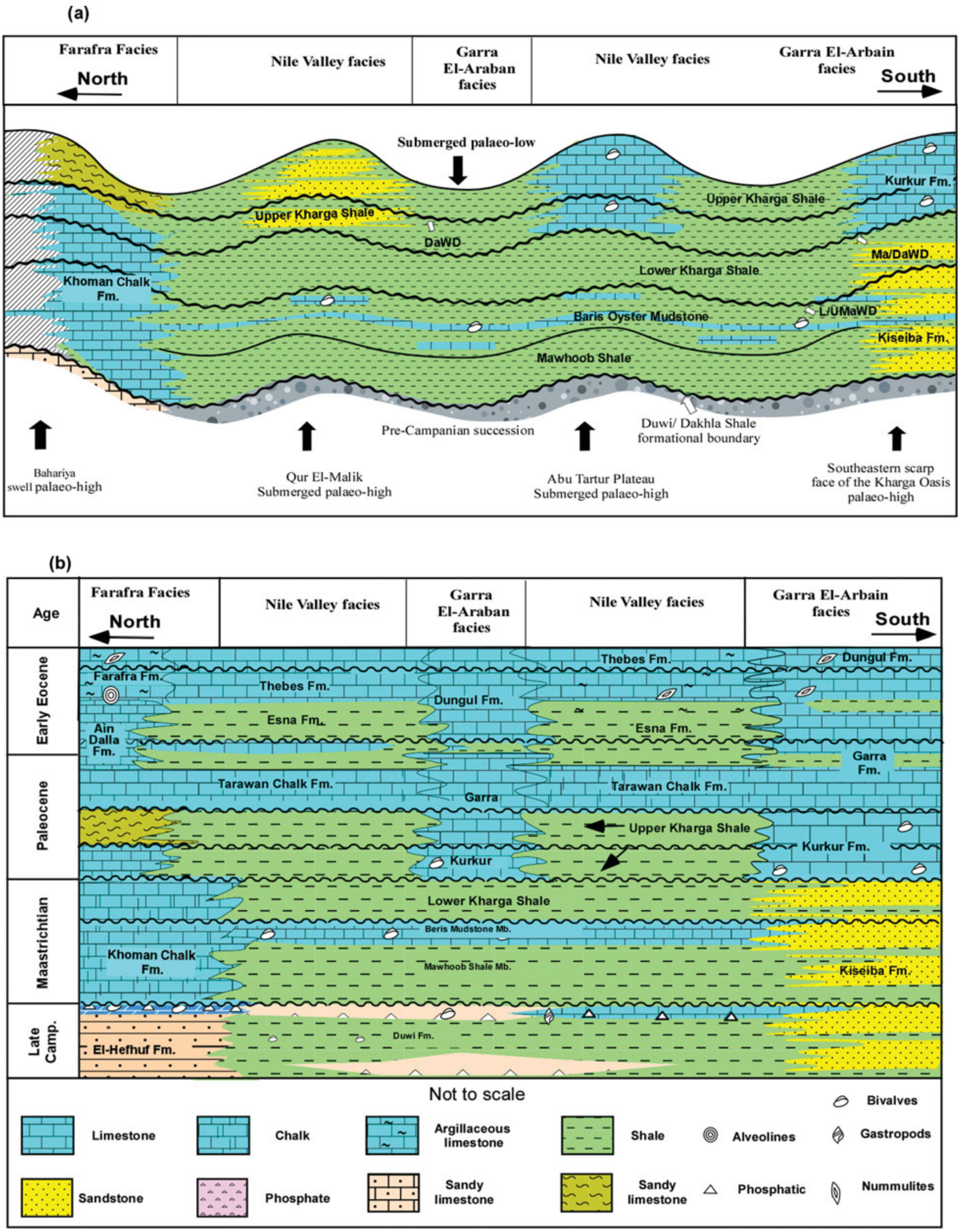

Figure 2. (Colour online) Facies variations and rock units in Western Desert, Egypt. (a) Three lateral and vertical facies changes in the Western Desert of Egypt are well known as Farafra , Nile Vally and the Garra El-Arbian facies. (b) The Cretaceous–Paleocene rock units exposed in the southern Western Desert of Egypt (after El-Azabi & El-Araby, 2000).

Samples 17–148 are barren of planktic foraminifera. However, following Tantawy *et al.* (2001), the Beris Mudstone Member (samples 80–147) is assigned to planktonic foraminiferal zones CF4–CF3 (see Fig. 4).

3.c. *Pseudoguembelina hariaensis* Zone (CF3)

This zone is defined as the biostratigraphic interval from the first appearance of *Pseudoguembelina hariaensis* Nederbraght to the last appearance of

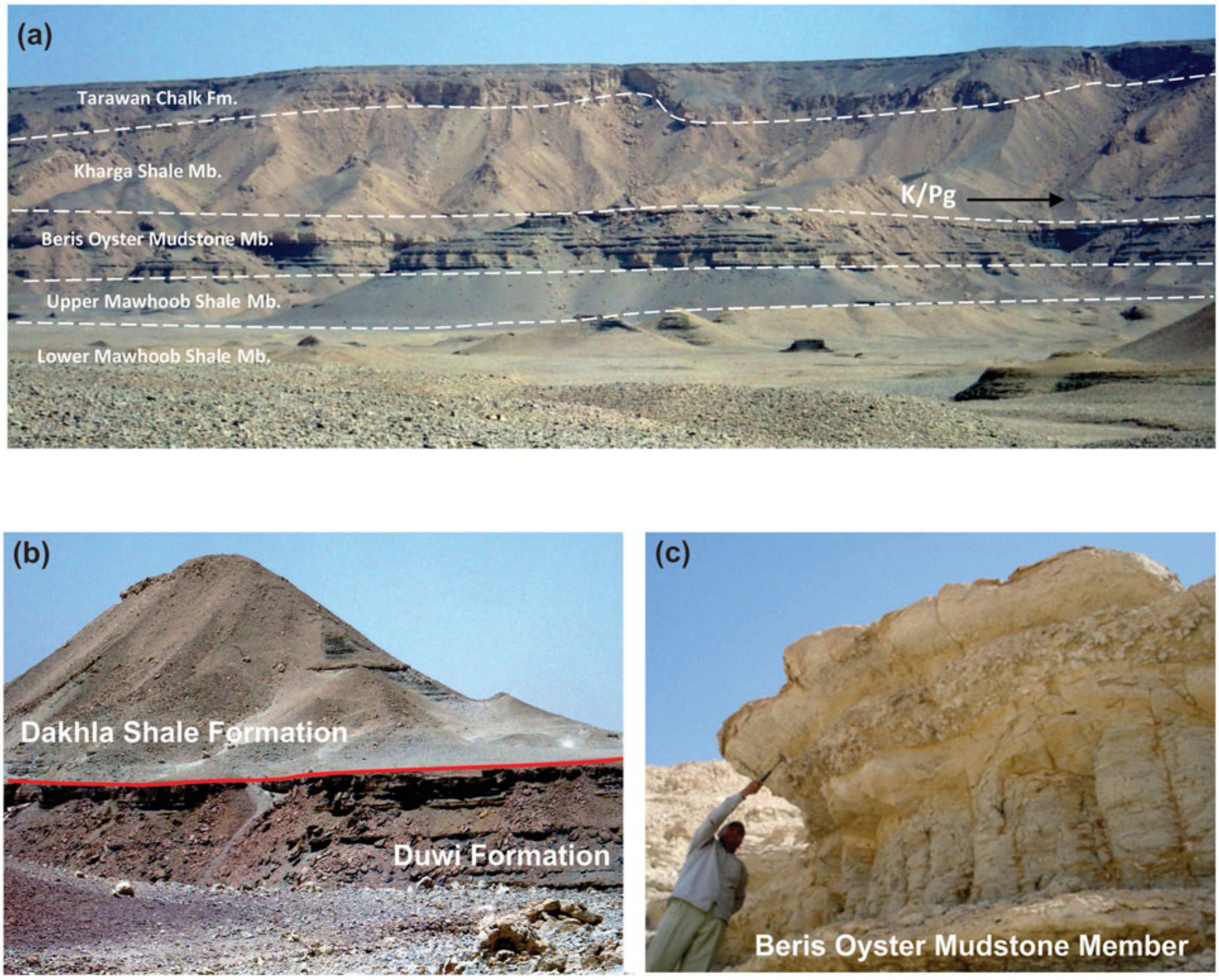

Figure 3. (Colour online) Field photographs. (a) General view of the Maastrichtian–Paleocene deposits in the eastern escarpment of the Dakhla Oasis, showing the three informal members (Mawhoob Shale, Beris Oyster Mudstone and Kharga Shale) of the Dakhla Formation, overlain by the carbonate platform of the Tarawan Formation. (b) The Duwi/Dakhla formational boundary. (c) Beris Oyster Mudstone Member marked by the abundance of the pelecypods, *Exogra overwegi*.

G. gansseri, recorded from the lower unit of the Kharga Shale Member (samples 148–165). The planktonic foraminiferal assemblage includes: *Racemiguembelina powelli* Smith and Pessagno, *Pseudoguembelina hariaensis*, *P. kempensis* Esker, *Rugoglobigerina reicheli* Brönnimann and *R. scotti* (Brönnimann) (see Fig. 4).

In the present study, the Lower Kharga Shale unit (samples 149–199) holds planktonic species that belong to Zone CF3. In fact, the top of Zone CF3 in most parts of Western Desert is marked by an erosional surface which is consistent with the K/Pg boundary identified by earlier workers (Abdel-Kirrem & Samir, 1995; Tantawy *et al.* 2001; Hewaidy, El-Azabi & Farouk, 2006; El-Azabi & Farouk, 2011; Farouk, 2016) (see Fig. 4).

3.d. *Globanomalina compressa* Zone (P1c)

This zone is defined from the last occurrence (LO) of *Globanomalina compressa* (Plummer) to the LO of *Praemurica uncinata* (Bolli) (see Fig. 4). This zone overlies the K/Pg unconformity, comprises *c.* 7 m of the upper unit of the Kharga Shale Member (samples 200–207) and is characterized by *Globanomalina compressa*, *Parasubbotina pseudobulloides* (Plummer), *P. variant* (Subbotina), *Subbotina triloculinoides* (Plummer), *Praemurica inconstans* (Subbotina) and *Chiloguembelina midwayensis* (Cushman). Earlier, Keller, Li & Macleod (1995) subdivided the P1c Subzone of Berggren *et al.* (1995) into P1c and P1d, based on the first occurrence of the *Praemurica trinidadensis* (Bolli). The presence of *P. trinidadensis* in this study interval is equated with the P1d Subzone of Keller, Li & Macleod (1995), Tantawy *et al.* (2001) and Keller *et al.* (2002) (Fig. 4).

3.e. *Praemurica uncinata* Zone (P2)

This zone is defined by the first appearance of *Praemurica uncinata* (Bolli) to the first appearance of *Morozovella angulata* (White). It occupies a part of the upper Kharga Shale Unit (samples 208–247, Fig. 4). The planktonic foraminiferal assemblage is similar to that of the underlying subzone except for the

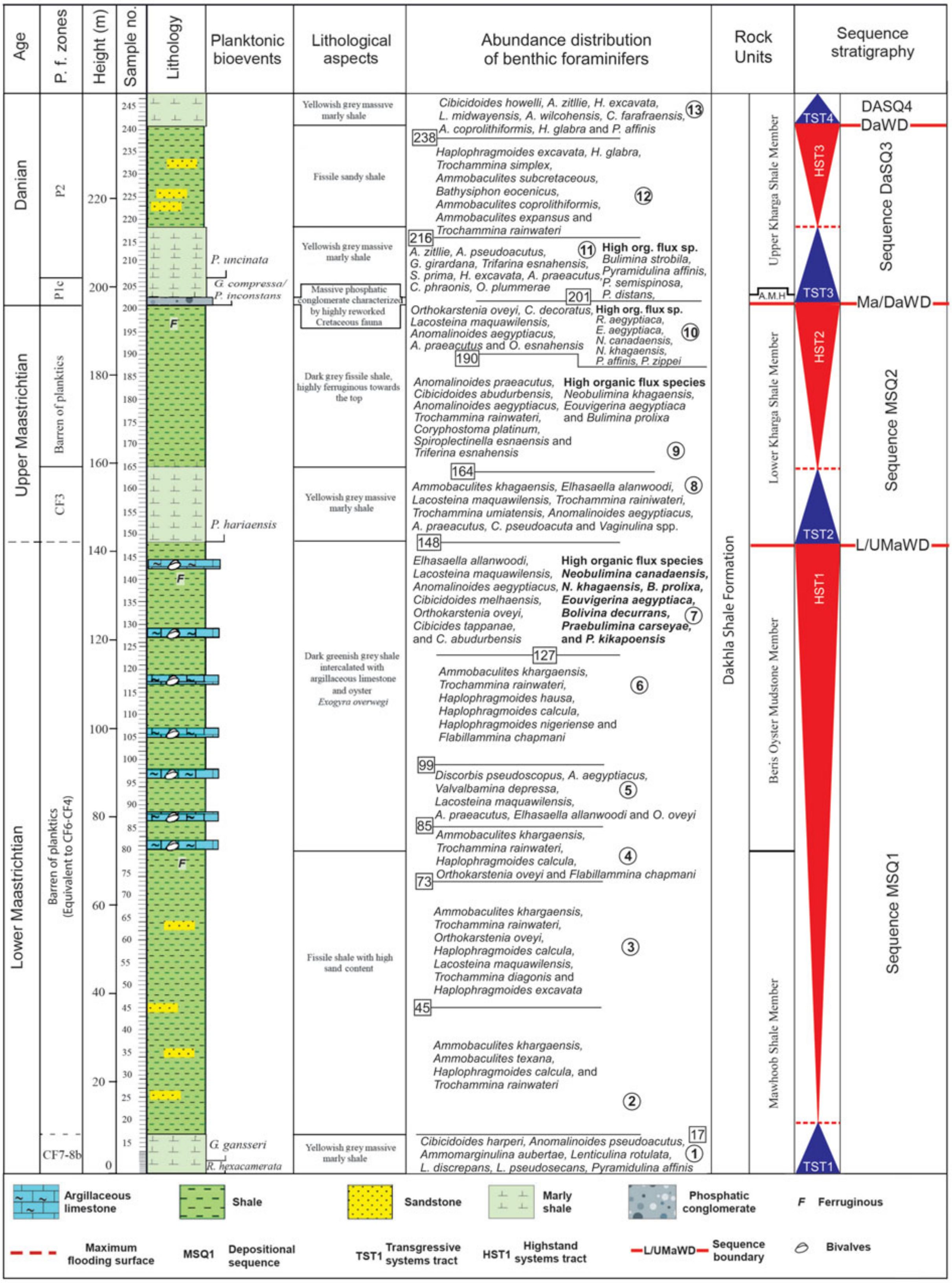

Figure 4. (Colour online) Biostratigraphy, benthic foraminiferal assemblage and sequence stratigraphy of the studied section.

first appearance of *Chiloguembelina subtriangularis* Beckmann, *Parasubbotina variospira* (Belford), *Morozovella praeangulata* (Blow), *Praemurica praecursoria* (Morozova) and *Praemurica uncinata* (Fig. 4).

4. Sequence stratigraphy

Four sequence boundaries are identified that are marked by sedimentation and faunal breaks (erosional, lack of biozones, reworking, facies shifts and sharp changes in biofacies) (see Fig. 4). These are named using an abbreviation of their assigned stage boundaries coupled with an abbreviation of the term Western Desert (Ca/MaWD, L/UMaWD, Ma/DaWD and DaWD) (Fig. 4). The inferred sequence boundaries in the Maastrichtian–Danian sediments document the presence of three third-order depositional sequences (El-Azabi & Farouk, 2010). They are named using the first letter of the assigned stage followed by an abbreviation of the term sequence with a running number counted separately for each stage (MSQ1, MSQ2, etc.). In all, three sequences are noted where each sequence represents a transgressive-regressive systems tract (TST-HST), where the lowstand systems tract (LST) are rarely initiated due to the deposition in an intra-shelf basin characterized by the presence of submerged palaeo-structural highs and lows (El-Azabi & Farouk, 2011). They are Sequence MSQ1 (TST1 and HST1), Sequence MSQ2 (TST2 and HST2), Sequence DaSQ3 (TST3 and HST3) and Sequence DaSQ4 (TST4) (Fig. 4; El-Azabi & Farouk, 2010).

4.a. Sequence MSQ1

This sequence comprises the Mawhoob Shale and Beris Oyster Mudstone members and covers the early Maastrichtian interval (see Fig. 4). It attains a thickness of *c.* 120 m. It is bounded at the base by the Campanian–Maastrichtian sequence boundary (Ca/MaWD) that unconformably separates the Duwi and Dakhla Shale formations (Fig. 3b; El-Azabi & Farouk, 2011). It coincides with a hiatus at the CF8a/CF8b zonal boundary, dated at 71 Ma (Li, Keller & Stinnesbeck, 1999) and close to the negative excursion of the Campanian–Maastrichtian Boundary Event (CMBE), well-recorded in different parts of the world (Voigt *et al.* 2012; Farouk, 2014). The sequence includes a transgressive systems tract (TST1), which is mainly composed of grey-greenish marly shale with siltstone intercalation, and a highstand systems tract (HST1), which consists of shale and sandy shale intercalated with abundant, low-diversity *Exogyra overwegi* argillaceous limestone (Fig. 4). The basal lowstand systems tract is missing due to the fast relative sea-level rise over the studied area, where the transgressive surface coincides with the sequence boundary at the Duwi–Dakhla Shale formational boundary (El-Azabi & Farouk, 2011; Fig. 4).

4.b. Sequence MSQ2

The upper Maastrichtian sequence (MSQ2) includes the Lower Kharga Shale Unit (Fig. 4). It has a thickness of *c.* 50 m. The precise age of sequence MSQ2 is hard to assign as its facies are barren of planktonic species or lie within the undifferentiated zones. In Dakhla, the lower part of this sequence is dated to Zone CF3. Sequence MSQ2, however, could be ascribed to late Maastrichtian zones CF4–CF3 (68.3–65.5 Ma) that typify the same interval in the deeper parts of the Dakhla Basin (Tantawy *et al.* 2001). This sequence is correlated with the upper part of the SQ3 sequence of Hewaidy, El-Azabi & Farouk (2006) and to DkSQ2 sequence of El-Azabi & Farouk (2011). The base of this sequence coincides with the lower–upper Maastrichtian boundary (= Beris Oyster Mudstone Member/Lower Kharga Shale Unit) and is characterized by a transition from shallow deposits to somewhat deeper neritic deposits in Kharga and Dakhla oases. The base of Sequence MSQ2 may be matched with a hiatus at the CF5/CF4 zonal boundary, which is dated at 68.3 Ma (Li, Keller & Stinnesbeck, 1999), and possibly with the global positive excursion of the Middle Maastrichtian Event (MME) (Voigt *et al.* 2012; Farouk, 2014). It is also close to the major cycle boundary KMa4 of Haq (2014) (Fig. 4). Sequence MSQ2 consists of foraminiferal marly shale with little shale and sand (samples 148–164) during the TST, followed upwards by ferruginous sandy shale barren of planktonic foraminifera during the HST (Fig. 4).

4.c. Sequence DaSQ3

The upper Danian sequence (DaSQ3) covers the lower and middle parts of the Upper Kharga Shale Unit (Fig. 4). It is bounded at the base by the K/Pg unconformity (Ma/DaWD) noted at 65.5 Ma and is characterized by the lack of planktic zones CF2–P1b (top of Zone CF3) (see Fig. 4). In the Dakhla–Kharga oases, it is easily defined as a horizon with a phosphatic conglomerate (*c.* 30 cm to 1 m thick) with crushed late Maastrichtian foraminifera called the Bir Abu Munqar Horizon (Barther & Herrmann-Degen, 1981; Farouk, 2016; Fig. 4). This horizon matches well with the K/Pg unconformity in Egypt and is marked by large time gap within Egypt's Western Desert due to tectonic uplift (Farouk, 2016; Fig. 4). This is followed by yellowish-grey massive foraminiferal marly shale during the TST, and above by a fissile shale during the HST (Fig. 4).

4.d. Sequence DaSQ4

This sequence is based on erosional surfaces, lithological and faunal assemblage changes and intensive reworking of older fauna during a new transgressive phase within the P2 Zone (TST4). The present study deals only with the lower part of this sequence.

5. Methods

A total of 13 232 specimens were analysed for benthic foraminiferal diversity, palaeoecology and palaeobathymetry from 247 samples of Maastrichtian–Danian deposits from a section at Dakhla Oasis at Gharb El-Mawohb at the main escarpment (26° 01′ 02″ N, 28° 13′ 18″ E; Fig. 1). Diversity measures (Shannon–Weaver information function known as Shannon *H*, Fisher's *α*, equitability *E* and dominance *D*) and

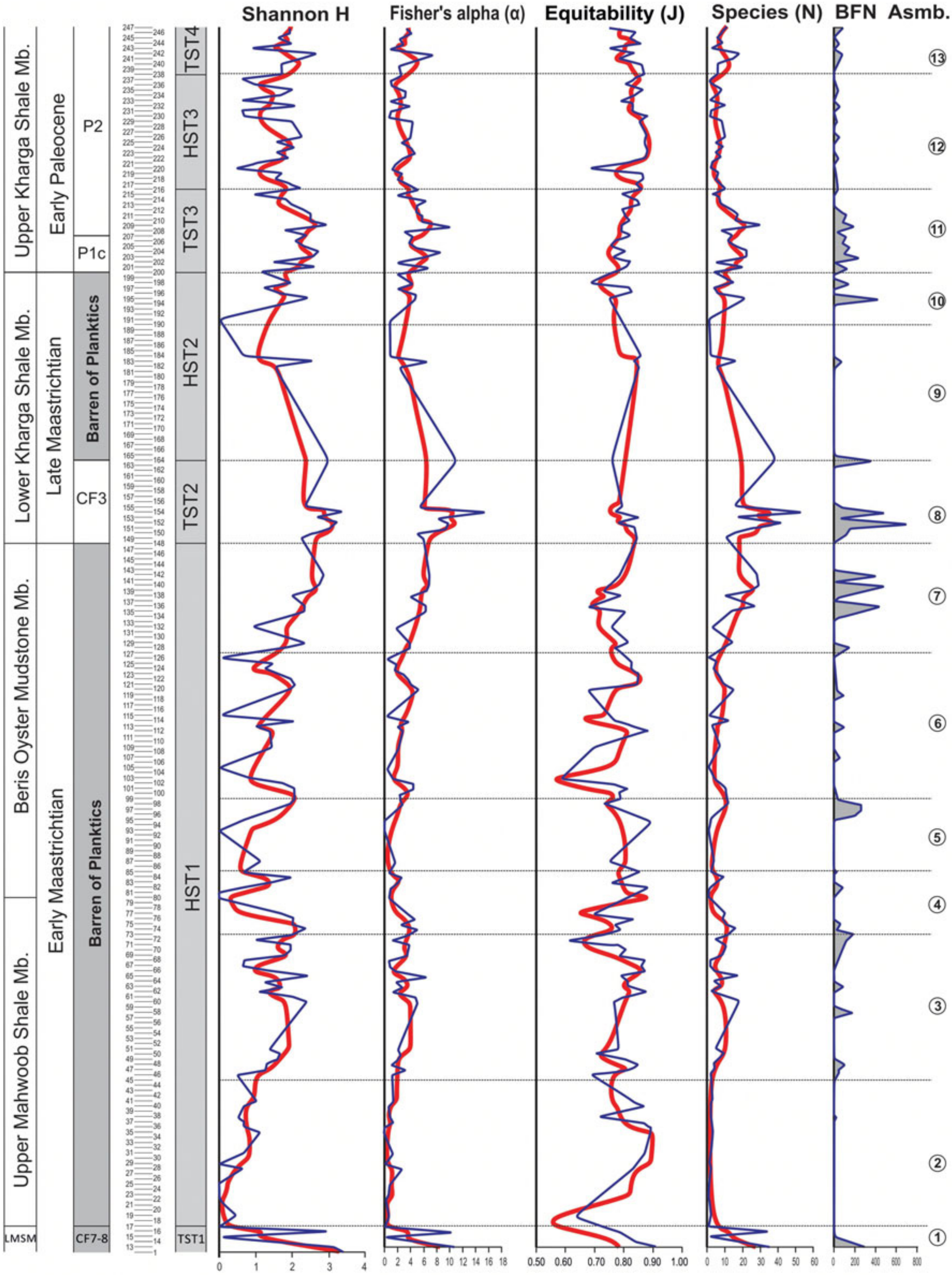

Figure 5. (Colour online) Diversity measures, species, BFN (benthic foraminifera numbers) and benthic foraminifera assemblages of the studied section. Bold lines (red) are 5-point running averages.

species abundance are used (Fig. 5). In combination, benthic foraminifera number (BFN) is used to infer changes in palaeooxygenation and organic matter flux. When inferred in conjunction with the BFN of dominant genera (*Trochammina*, *Haplophragmoides* and *Ammobaculites*) and species (i.e. *Ammobaculites khargaensis* Nakkady and Talaat and *Elhasaella allanwoodi* Hamam) (Fig. 6), they provide a robust estimation of the prevailing palaeoenvironment (Bernhard, 1987; Kaiho & Hasegawa, 1994; Jorissen, De Stigter & Widmark, 1995; Van der Zwaan *et al.* 1999; Murray, 2000; Holbourn, Kuhnt & Erbacher, 2001; Herrle *et al.* 2003*a*, *b*). Diversity measures (Shannon *H*, Fisher's *α*, equitability and dominance) are further used to

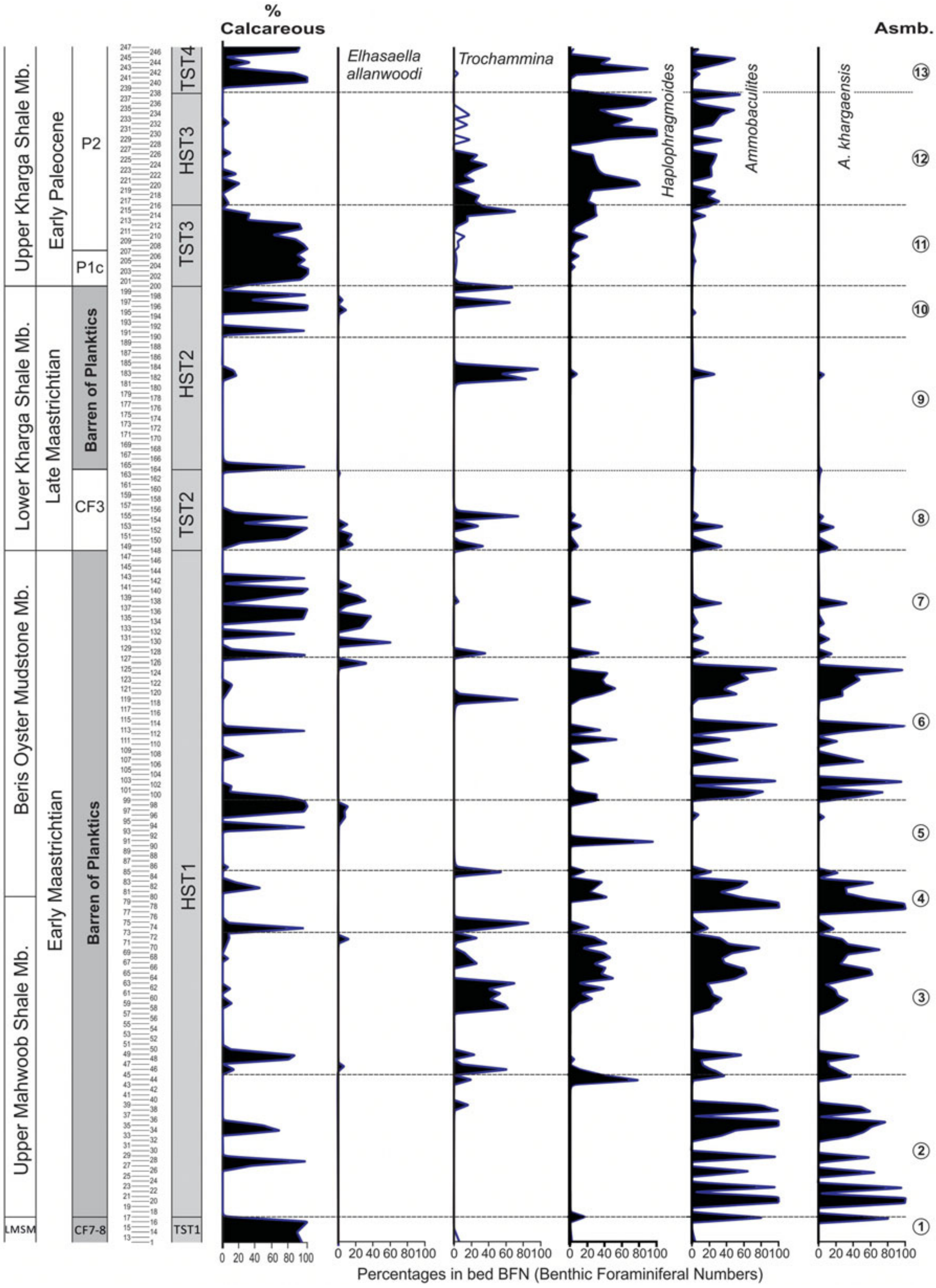

Figure 6. Distribution of dominant benthic foraminiferal species and genera in the studied section.

provide a better estimation of the prevailing ecological structure and depositional environment (Figs 7, 8).

Faunal change before and after the Cretaceous–Palaeogene boundary (K/Pg, also known as the Cretaceous–Tertiary boundary or K/T) is also addressed (Figs 9, 10). The pre- and post-K/Pg distribution of high-organic-flux benthic foraminiferal species is also analysed for a better understanding of the prevailing environment in terms of changes in nutrient availability (Table 1). The temporal species distribution (calcareous v. agglutinated) with respect to TST/HST is also provided (Fig. 11).

All data are summarized (Fig. 12) and interpreted in terms of sequence stratigraphy, regional tectonics,

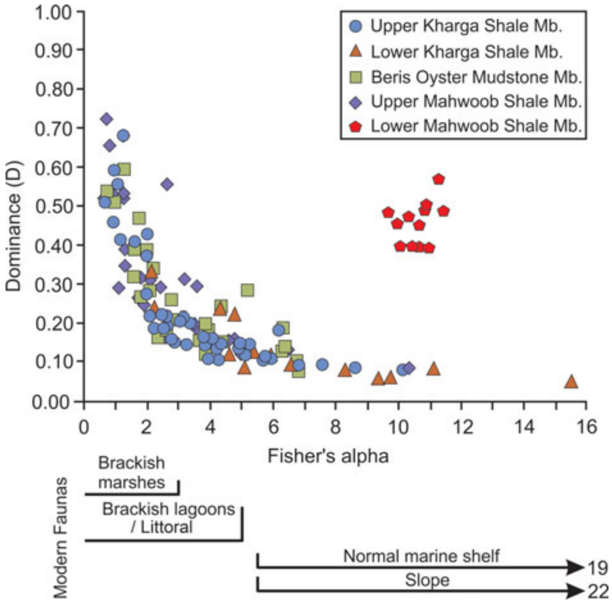

Figure 7. (Colour online) Benthic foraminiferal depositional settings categorized by stratigraphic members.

climate and sea level (Fig. 13). The inferred sea level is based on the abundance (%) pattern of calcareous benthic foraminifera, species abundance, distribution of characteristic species, lithology and the presence (P/B ratio) and absence of planktonic foraminifera. The palaeodepth followed here includes: Inner Neritic: <50 m; Middle Neritic: 50–100 m; Outer Neritic: 100–200 m; and Bathyal >200 m.

6. Results

6.a. Species diversity, BFN, P/B ratios and depositional setting

A statistically significant correlation (Pearson = 0.916 at the 0.01 level; 2-tailed) is noted between Fisher's α and Shannon H, suggesting that both indexes are good proxies for species diversity (Table 2). Fisher's α, a within-habitat diversity index and a preferable proxy for species diversity, considers both evenness and richness; other species abundance models consider only evenness, however. A statistically significant and positive correlation (Pearson = 0.741 at the 0.01 level; 2-tailed) is also noted between Fisher's α and BFN (Table 3), broadly suggesting that increased oxygenation of the bottom waters and the availability of organic matter flux (= higher BFN numbers) has a strong correlation with increased species diversity. Dominance (D) and Fisher's α shows a negative relationship, suggesting that high dominance is marked by low diversity (Fig. 7).

6.a.1. Highstand systems tracts

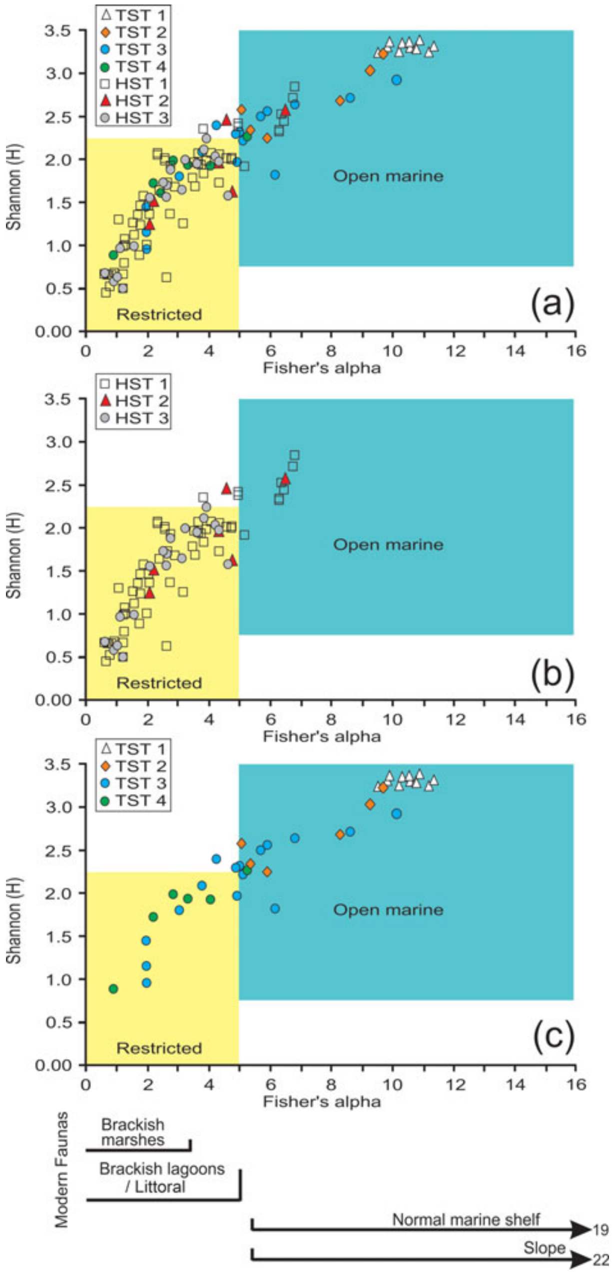

Figure 8. (Colour online) Sequence stratigraphic-based benthic foraminiferal community structure and depositional settings. The plot of Fisher's α versus Shannon H gives a good idea of the depositional settings (i.e. restricted v. open marine) of the studied sequence-based benthic foraminiferal fauna. (a) All; (b) HST; and (c) TST dataset.

Three highstand systems tracts (HST) are identified (Figs 5, 12; Table 3): HST1 (samples 18–148; assemblages 2–6); HST2 (samples 164–200; assemblages 9–10); and HST3 (samples 216–238; assemblage 12). During HST1 all diversity indices and BFN steadily increase, but the values remain at low–moderate levels (Fig. 5). HST1 is also marked by the absence of planktonic foraminifera except in a very few samples that have very low P/B ratios (<5 %). HST2 is marked by declining values of all diversity measures and BFN (Fig. 5), along with the absence of planktonic foraminifers. HST3 displays low species diversity and BFN along with the absence of planktonic foraminifers (P/B ratio = 0; Fig. 5). Both HST1 and HST2 fauna sit largely within the restricted brackish lagoonal/littoral region with few

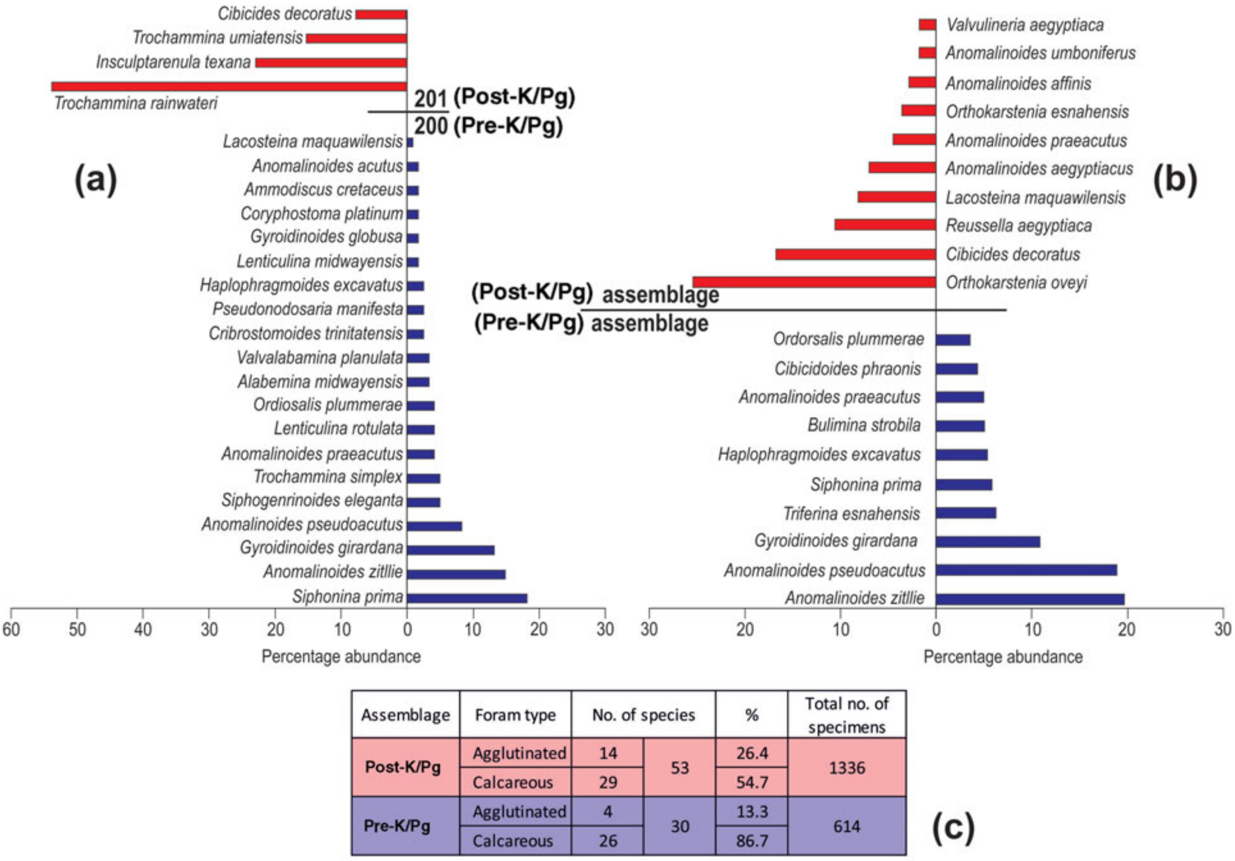

Assemblage	Foram type	No. of species		%	Total no. of specimens
Post-K/Pg	Agglutinated	14	53	26.4	1336
	Calcareous	29		54.7	
Pre-K/Pg	Agglutinated	4	30	13.3	614
	Calcareous	26		86.7	

Figure 9. (Colour online) Changes from pre-K/Pg to post-K/Pg (a) between samples 200 and 201; (b) in assemblages 10 and 11; and (c) in numbers.

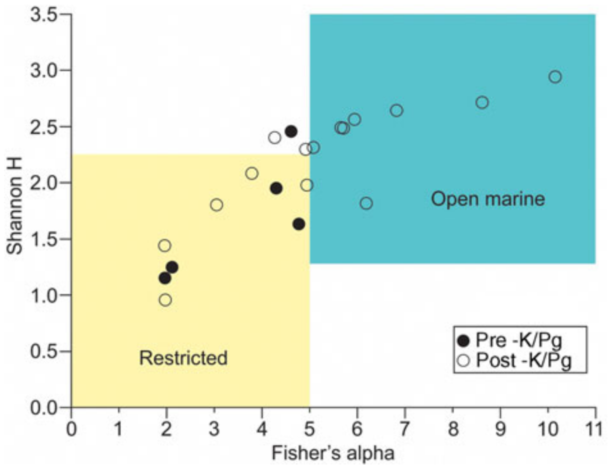

Figure 10. (Colour online) Plot of Fisher's α versus Shannon H of assemblages 10 (pre-K/Pg) and 11 (post-K/Pg) showing the depositional settings (i.e. restricted v. open marine).

data points transgressing into the open marine region, whereas those of HST3 fall within the restricted brackish littoral region (Fig. 8).

6.a.2. *Transgressive systems tracts*

Four transgressive systems tracts (TST) are identified (Figs 5, 12): TST1 (samples 1–17; assemblage 1); TST2 (samples 127–164; assemblages 7–8); TST3 (samples 201–216; assemblage 11); and TST4 (samples 238–247; assemblage 13). TST1 is marked by maximum diversity and moderate BFN values and with high P/B ratio (50–70 %) (Figs 5, 12). TST2 is characterized by moderately high P/B ratios (25–60 %) with peak diversity values that begin to decline midway; the BFN values are also the highest recorded (Figs 5, 12). TST3 is marked by the presence of high diversity values, BFN and percentage calcareous benthic foraminiferal species with a P/B ratio ranging over 50–70 %. TST4 is characterized by moderate values of species diversity, BFN and percentage calcareous benthic foraminiferal species and with P/B ratio ranging over 50–65 % (Figs 5, 12). Both TST1 and TST2 data points fall well within the open marine region (Fig. 12). TST3 data points largely plot in the open marine region, but also transgress into the restricted brackish littoral region (Fig. 8).

6.b. Benthic foraminiferal assemblage

6.b.1. *Highstand systems tracts*

In HST1, the agglutinated taxa (*Ammobaculites*, *Haplophragmoides* and *Trochammina*) are well distributed throughout, especially *Ammobaculites khargaensis* (Fig. 6). Seven benthic foraminiferal assemblages

Table 1. Distribution of high-flux species (see text for explanation) in the studied section with an emphasis on their pre- (lower) and post- (upper, shaded) K/Pg distribution.

Pyramidulina affinis	*Pyramidulina zippei*	*Pyramidulina vertebralis*	*Pyramidulina distans*	*Praebulimina carseyae*	*Neobulimina canadaensis*	*Eouvigerina aegyptiaca*	*Reussella aegyptiaca*	*Neobulimina khagaensis*	*Praebulimina kikapoensis*	*Bulimina prolixa*	*Bolivina decurrans*	*Praebulimina russi*	*Bulimina strobila*	*Pyramidulina semispinosa*	Total BFN	% of total BFN	Cycles
16	16	13	3												48	5	TST4
17			4										56	5	82	9	TST3
7	2				8	5	65	11		1					99	11	HST2
26	23	8	10	61	103	21		50	26		13	8			349	38	TST2
										18					18	2	HST1
138				134		47									319	35	TST1

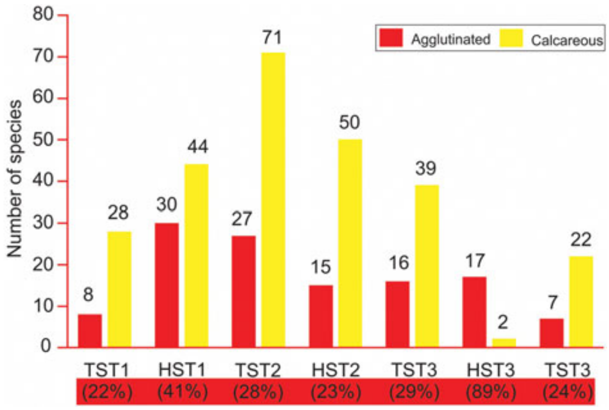

Figure 11. (Colour online) Distribution of benthic foraminiferal species with respect to identified HST and TST sequences. The bottom highlighted part shows the percent of agglutinated benthic foraminiferal species within each cycle.

are inferred (assemblages 2–7) that are dominated by agglutinated forms (especially *A. khagaensis*), except in assemblages 5 and 7 that are marked by the dominance of calcareous forms, *Discorbis pseudoscopos* Nakkady and *Elhasaella alanwoodi*, respectively (see Fig. 12). HST2 has two benthic foraminiferal assemblages (assemblages 9–10) and is marked by the presence of high-organic-flux species (*Neobulimina canadaensis* Cushman and Wickenden, *N. khagaensis* Nakkady and Talaat, *Bulimina prolixa* Cushman and Parker, *Eouvigerina aegyptiaca* Nakkady, *Bolivina decurrans* (Ehrenberg), *Praebulimina carseyae* (Plummer), *P. kikapooensis* (Cole), *Pyramidulina affinis* (Hantken) and *P. zippei* Reuss). Assemblage 9 is marked by the dominance of shallow-water agglutinated taxa of *Trochammina* (*T. rainwateri* Cushman and Applin, *T. diagonis* (Carsey) and *T. umiatensis* Tappan) and assemblage 10 by slightly deeper water calcareous taxa, *Orthokarstenia oveyi* (Nakkady) and *Cibicidoides decoratus* (Le Roy), with accessory *Reussella aegyptiaca* Nakkady and *Lacosteina maquawilensis* Ansary and Fakhr (Fig. 12). HST3 is marked by the dominance of agglutinated *Haplophragmoides*, with accessory *Ammobaculites* and *Trochammina* (Figs 6, 12).

6.b.2. *Transgressive systems tracts*

All TSTs are marked by the dominance of calcareous forms: TST1 by *Cibicidoides harperi* (Sandidge) and *C. pseudoacutus* (Nakkady); TST2 by *Elhasaella alanwoodi* and *Lacosteina maquawilensis* Ansary and Fakhr; TST3 by *Anomalinoides zitllie* (Le Roy), *Cibicidoides pseudoacutus* and *Gyroidinoides girardana* (Reuss); and TST4 by *Cibicidoides howelli* (Toulmin) and *Anomalinoides zitllie* (Fig. 12).

6.c. Cretaceous–Palaeogene boundary (K/Pg)

The Cretaceous–Palaeogene boundary (K/Pg) is noted between samples 200 and 201 (Figs 9, 10, 12). The changes in diversity and species composition are marked (Figs 9, 10, 12). Post-boundary (beyond sample 200) is characterized by short fluctuations and the dominance of *Haplophragmoides* (Figs 6, 12). Assemblage-wise, both the number of species and specimens increase post-boundary (Fig. 9) and all pre-boundary data points plot in the restricted area (Fig. 10). Species-wise, only the middle neritic species *Anomalinoides aegyptiacus* transgresses the boundary (Fig. 9) and assemblage-wise, very few genera (30 %) are able to transgress the boundary (Table 4).

6.d. High-organic-flux species

The high-organic-flux benthic foraminiferal species provide a rough estimate of the availability of nutrients within the environment. Their distribution (Table 1) provides a window to their response to changes in nutrient availability within the marine realm. These high-organic-flux species include *Pyramidulina affinis*, *Pyramidulina zippei*, *Pyramidulina vertebralis* (Batsch), *Pyramidulina distans* (Reuss), *Praebulimina carseyae*, *Neobulimina canadaensis*, *Eouvigerina*

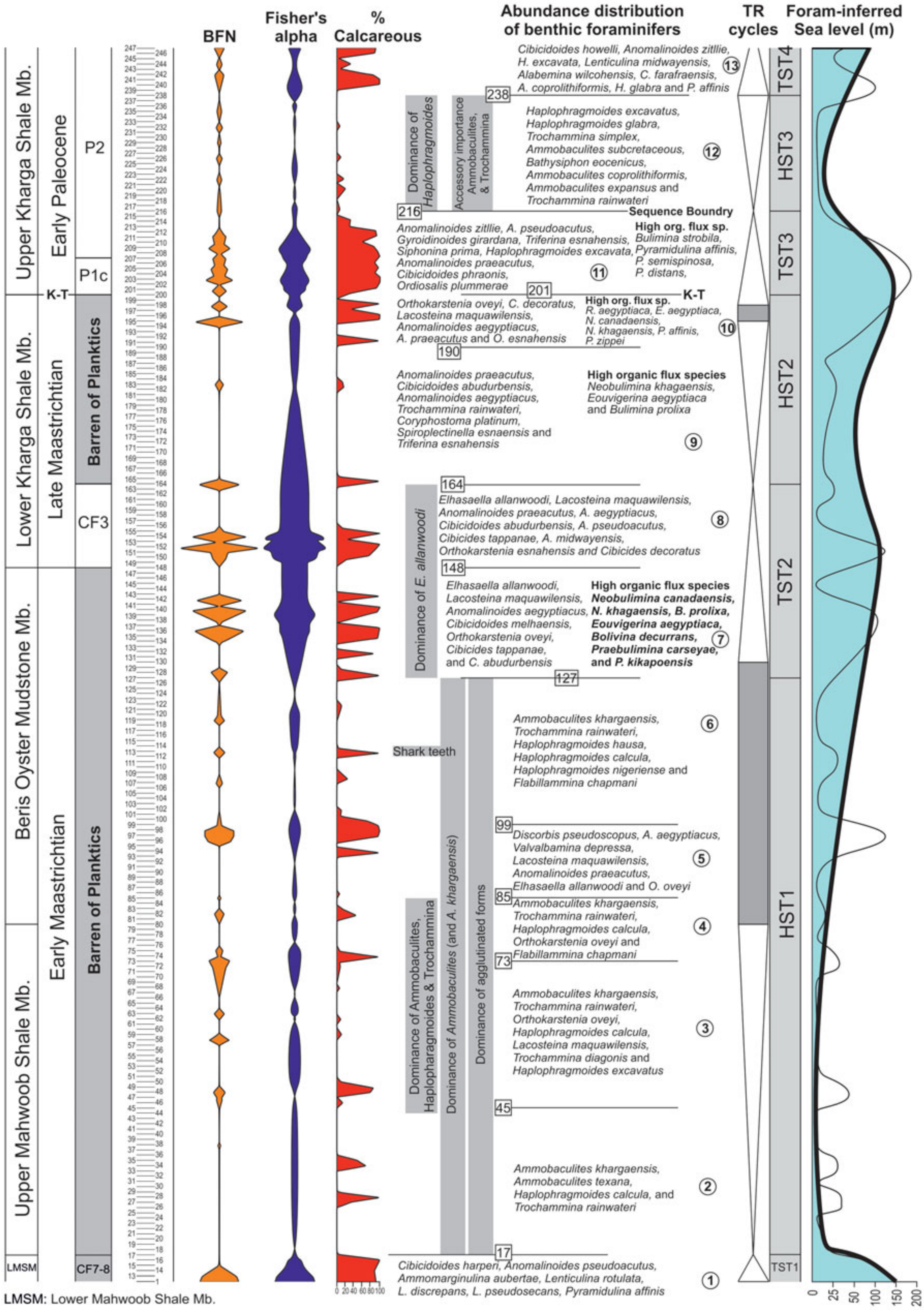

Figure 12. (Colour online) Summary of event and the inferred sea-level curve of the studied Maastrichtian–Danian sediments. See text for palaeodepth parameters used to infer the present sea-level curve.

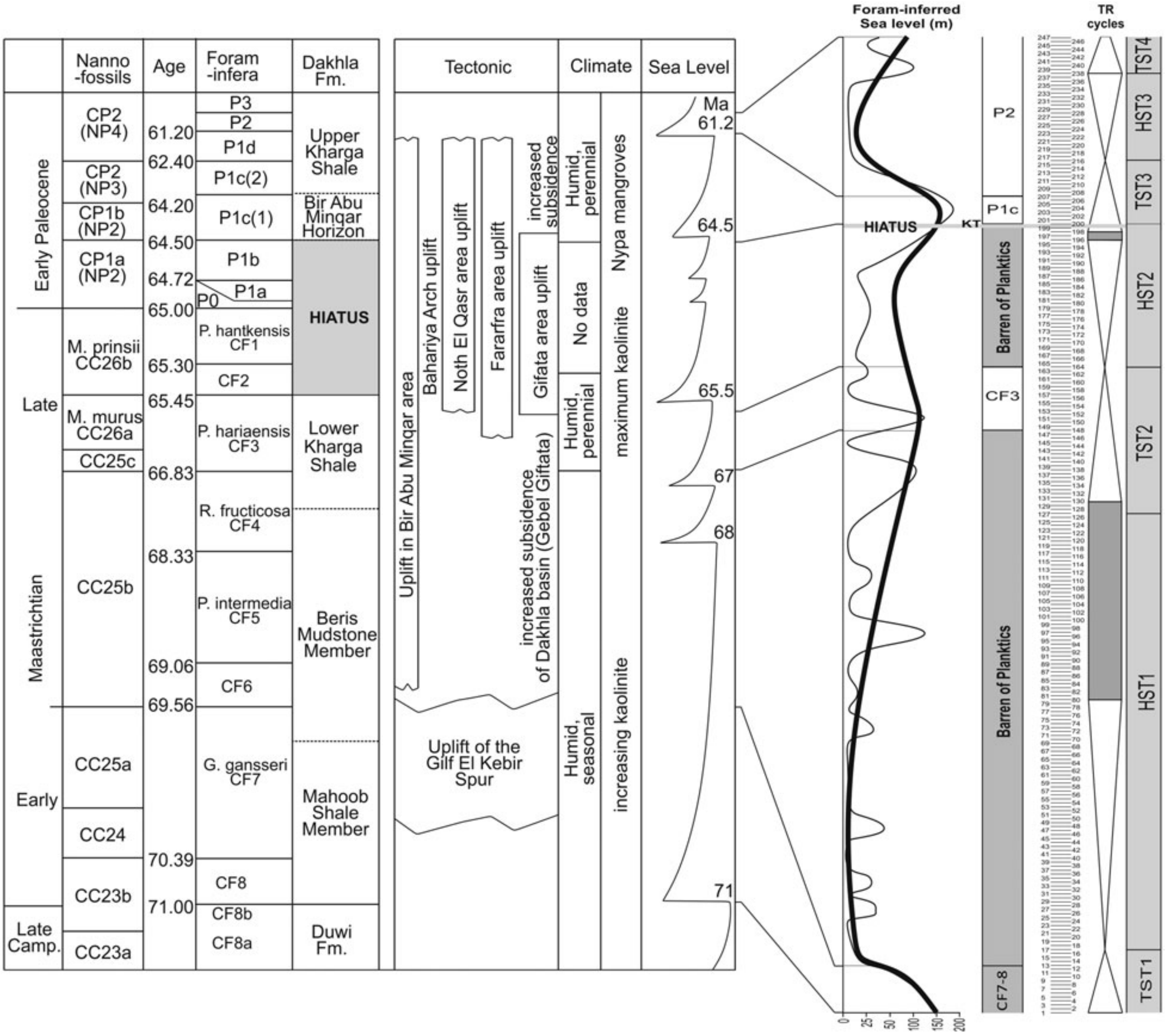

Figure 13. Correlation of regional tectonics, climate and sea-level changes (after Li, Keller & Stinnesbeck, 1999; Tantawy *et al.* 2001) and inferred sea-level curve of the studied Maastrichtian–Danian sediments.

aegyptiaca, *Reussella aegyptiaca*, *Neobulimina khagaensis*, *Praebulimina kikapooensis*, *Bulimina prolixa* Cushman and Parker, *strobila* Marie, *Bolivina decurrans*, *Praebulimina russi* and *Pyramidulina semispinosa* (Le Roy) within the studied section. In the present study, the pre-K/Pg TST and the pre-K/Pg duration are marked by a higher abundance of organic-flux species (Fig. 10). *Praebulimina*, *Neobulimina*, *Eouvigerina*, *Reussella* and *Bolivina* (all bi/tri-serial and thick-shelled/heavily ornamented forms) do not cross the K/Pg boundary, whereas *Pyramidulina* and *Bulimina* transgress the boundary (particularly the former; Table 1).

A summary of all proxies, percent calcareous foraminifera, benthic foraminiferal assemblage and inferred bathymetry (relative sea level) is given in Fig. 12. Bathymetry (relative sea level) is inferred by using the presence of characteristic species, the abundance values of calcareous benthic foraminifers and the presence and abundance of planktonic foraminifers. Taken together, these proxies provide a sound estimate of the relative sea level (Figs 12, 13).

7. Discussion

The most striking feature of this Maastrichtian–Danian section is the overall abundance of benthic foraminiferal species (156) and the fact that even the most dominant species do not go beyond 6 % of the total benthic assemblage (13 232 specimens; 129 species do not go beyond 1 %), that is, displaying a remarkably high level of equitable environment (Fig. 5). This is all the more interesting since many of the data points plot in the restricted lagoonal/littoral environment (mostly brackish and some in normal marine lagoons), rather than the normal marine environment (Figs 7, 8) as would be expected with high species diversity (Fig. 12). Additionally, in spite of the shallow and restricted depositional settings, the fauna is not stressed as even the HST fauna shows

Table 2. A statistically significant correlation is noted between diversity measures, Fisher's α and Shannon H.

		Fisher's α	Shannon H
Fisher's α	Pearson correlation	1	0.916*
	Significant (2-tailed)		0
	N	144	135
Shannon H	Pearson correlation	0.916*	1
	Significant (2-tailed)	0	
	N	135	138

*Correlation is significant at the 0.01 level (2-tailed).

Table 3. A statistically significant correlation is noted between Fisher's α and BFN (benthic foraminifera numbers).

		Fisher's α	BFN
Fisher's α	Pearson correlation	1	0.741*
	Significant (2-tailed)		0
	N	144	144
BFN	Pearson correlation	0.741*	1
	Significant (2-tailed)	0	
	N	144	151

*Correlation is significant at the 0.01 level (2-tailed).

Table 4. Distribution of benthic foraminiferal genera. The upper shaded part shows the occurrence of genera present during both pre- and post-K/Pg time.

Pre-K/Pg assemblage	Post-K/Pg assemblage
Ammobaculites	
Anomalinoides	
Bulimina	
Lacosteina	
Orthokarstenia	
Pyramidulina	
Trifarina	
Trochammina	
Valvalbamina	
	Alabamina
	Ammodiscus
	Ammomarginulina
	Bathysiphon
Cibicides	
	Cibicidoides
	Coryphostoma
	Cribrostomoides
Discorbis	
Elhasaella	
Eouvigerina	
	Frondicularia
	Gavelinella
	Gyroidinoides
	Haplophragmoides
Insculptarenula	
	Laevidentalina
	Lenticulina
	Marginulinopsis
Neobulimina	
	Nodosaria
	Oridorsalis
	Osangularia
	Pseudonodosaria
Reussella	
	Siphogeneroides
	Siphonina
	Tappanina
Vaginulina	
Valvulineria	

a moderate to high percentage of calcareous benthic foraminifers (except for HST3; see Figs 11, 12).

In modern faunas, Fisher's α values below 5 (restricted region) characterize environments where the restricting factor is low salinity such as in estuary and hyposaline lagoons (Murray, 1973, 2006), in modern hypoxic estuarine waters (fjord environments; Alve & Nagy, 1986; Nagy & Alve, 1987; Alve, 1990) and in the Triassic–Jurassic organic-rich shales (Nagy, Løfaldi & Bäckström, 1988; Nagy, Pilskog & Wilhelmsen, 1990; Nagy, Hess & Alve, 2010). Interestingly, the present data also largely (especially the HST fauna) plot in the restricted region (see Fig. 8; 70 % of the present data is <5, Fisher's α). Previous sea-level data (see Li, Keller & Stinnesbeck, 1999; Tantawy *et al.* 2001) also suggest that during the studied period, humid (seasonal or perennial) conditions prevailed which would have had led to increased runoff and therefore a greater influence of freshwater (low salinity) on the benthic fauna (especially during HSTs; regressive phase) (see Fig. 13). Increased runoff and concomitant shallowing would also explain the higher sand content during HST1 and HST3 (Fig. 4) and the resultant dominance of agglutinated *Ammobaculites*, *Haplophragmoides* and *Trochammina* throughout the studied section. Conditions of largely oligotrophic (*Ammobaculites*) and moderate (?) to low oxygen (*Haplophragmoides* and *Trochammina*) in brackish marginal marine waters and marsh settings are therefore envisioned. A similar association of *Ammobaculites*, *Haplophragmoides* and *Trochammina* has been interpreted to belong to marsh or littoral conditions with reduced salinity and, in warm climates, with increased precipitation and terrestrial runoffs (Luger, 1988; Keller *et al.* 2002). Shallowing is further corroborated by the prevailing benthic species that are mostly characteristic of shallow waters (middle neritic; <100 m) such as *Ammobaculites*, *Haplophragmoides*, *Trochammina*, *Orthokarstenia*, *Anomalinoides*, *Bulimina*, *Lenticulina* and *Cibicidoides* with few open marine incursions (mostly middle to outer neritic forms; <200 m) of *Cibicides*, *Bolivina*, *Eouvigerina*, *Praebulimina* and *Gyroidinoides* in assemblages 1, 5, 7, 9–11 and 13 (see Fig. 12).

Much of the early Maastrichtian period was one of low species diversity (but increasing gradually) dominated by agglutinated forms, in largely oligotrophic, moderate (?) to low oxygen conditions of a brackish marginal marine or marsh settings. However, at the end of the early Maastrichtian Age, the dominance of calcareous forms (*Elhasaella*, *Cibicides*, *Cibicidoides*) and high-organic-flux species (*Bolivina*, *Eouvigerina*, *Praebulimina* and *Bulimina*) suggest marine incursion and possibly upwelling (high palaeoproductivity; = assemblage 7) in otherwise restricted littoral settings; possible upwelling is also the case for the upper Maastrichtian HST2, which also displays an increased presence of high-flux species.

On the other hand, the TST (TST1–4) fauna, especially TST1 (Campanian) and TST4 (Danian) (see also

Fig. 12), is also marked by considerably deeper conditions (middle to ? outer neritic) as reflected by the presence of marly shales (Fig. 4); this is similar to the case in the lower part of the upper Maastrichtian sediments (Fig. 4).

Additionally, most of the identified sequence boundaries (see Fig. 4) correlate well with the boundaries detected in the Eastern Desert, Sinai Peninsula, Jordan, Tunisia, Libya, Arabian Plate, Western Europe and the New Jersey continental margin (Haq, Hardenbol & Vail, 1987; Hardenbol *et al.* 1998; Li, Keller & Stinnesbeck, 1999; Miller *et al.* 2005; Molina *et al.* 2006; Sebei *et al.* 2007; Farouk, 2014, 2016; Farouk, Marzouk & Fayez, 2014). The Arabian Platform has experienced a complex tectonic history in addition to being widely influenced by eustatic sea-level changes (Haq & Al-Qahtani, 2005); both tectonics and eustasy have played important roles in the development of sedimentary sequences and the intervening hiatuses (Farouk, 2015). The boundary Ma/DaWD, however, is marked by a long period of hiatus in sedimentation. Other boundaries identified in the present work have no correspondences in the Arabian Platform-wide cycle charts of Haq & Al-Qahtani (2005). In the present study, the KM5 and PaDa1 major cycle boundary of Haq (2014) may be correlated in the present study with the Ma/DaWD sequence boundary (see Fig. 4) due to erosional surface across the K/Pg unconformity.

7.a. Cretaceous–Palaeogene boundary (K/Pg)

The Cretaceous–Palaeogene boundary (K/Pg) is noted between samples 200 and 201 and between assemblages 10 and 11 (see Figs 9, 12). The dramatic change in fauna and the fact that none of the species persist beyond the boundary, between samples 200/201 (Fig. 9a), suggests a possible in-between hiatus. A broader view (of assemblages) is therefore taken to better understand changes from pre-K/Pg to post-K/Pg (Fig. 9b). Fundamentally, there is improvement in the environment after the K/Pg boundary in terms of diversity, number of species and specimens (Fig. 9c). *Anomalinoides aegyptiacus*, a characteristic middle neritic benthic species, transgress the boundary, suggesting not much change in palaeodepth from pre-K/Pg to post-K/Pg (Fig. 9).

As well as palaeodepth (mostly a local parameter), two major global ‘signals’ have been noted for differences after the K/Pg boundary: (1) a sudden drop in productivity (surface and bottom) and (2) reduced bottom water oxygenation followed by a gradual faunal recovery during Danian time (early Paleocene; see also Speijer *et al.* 1996). Present data suggest that in the post-K/Pg duration (Danian), there is a reduction in the abundance of high-organic-flux species (i.e. bi-/tri-serial morphogroups), suggesting a shift from more mesotrophic open marine environment (assemblage 10) to a much reduced oligotrophic condition (=assemblage 11; Fig. 13; Table 1). For higher numbers of species, BFN and diversity measures (Figs 5, 12) also indicate that neither oxygen nor nutrient availability was a deterrent in the post-boundary duration (assemblage 11; Fig. 12).

Tn the present study, the immediate post-K/Pg duration is characterized by increased species diversity, number of species and specimens in a more oligotrophic environment with little change in palaeobathymetry.

7.b. Sea-level curve

The inferred sea-level curve based on the use of characteristic benthic foraminiferal species, their abundance values (%) and the presence and abundance of planktonic foraminifers (P/B ratio) (see Figs 12, 13) replicates the regional sea-level curve of Li, Keller & Stinnesbeck (1999) and Tantawy *et al.* (2001). High sea level persisted during late Campanian time, followed by a sudden shallowing and a gradual increase throughout early Maastrichtian time (Figs 12, 13). The early Maastrichtian Age was largely a period of tectonic quiescence and of subsidence in a warm, wet, tropical and subtropical setting characterized by low seasonality contrasts (based on kaolinite conten; see also Keller *et al.* 2002) (Figs 12, 13). The late Maastrichtian regional tectonic activity and maximum kaolinite content indicates a higher but receding episodic sea-level trend (Fig. 13). The lowest Danian deposits (Zone P1c) record the highest sea level, humid perennial conditions and increased regional subsidence (Fig. 13). The succeeding Danian P2 Zone is marked by a rapid fall in sea level and of tectonic quiescence (Fig. 13).

It therefore appears that the inferred sea-level curve is much more influenced by the prevailing climate and global eustasy as opposed to regional tectonics (Fig. 13). Benthic foraminifera seem to reflect changes in sea level, and are a potential tool in interpreting regional sequence stratigraphy.

8. Conclusion

Maastrichtian–Danian benthic foraminiferal assemblages are analysed with respect to sequence stratigraphy (in terms of HST and TST). Overall, data suggest a remarkably highly equitable environment. Much of the data plot in the restricted littoral environment (mostly brackish and some in normal marine lagoons) rather than the normal marine environment, as would be expected with a high-diversity dataset, suggesting that the fauna are not stressed despite a shallow depositional setting. The dominance of agglutinated taxa indicates moderate (?) to low oxygen conditions in a brackish littoraland/or marsh settings with reduced salinity, possibly due to increased precipitation and terrestrial runoff. The interrupted dominance of calcareous forms and high-organic-flux species suggest occasional marine incursions and high palaeoproductivity due to local upwelling. The inferred sea-level curve from benthic foraminifera replicates the regional sea-level curve, and suggests that (1) the curve is more influenced by the prevailing climate and global eustasy rather than by regional tectonics and (2) benthic foraminifers seem to be a good proxy for evaluating sea-level changes. The post-Cretaceous–Palaeogene boundary indicates an improvement in the environment in terms of diversity, number of species and specimens with a marked reduction in the abundance of high-organic-flux species, indicating a shift from a more mesotrophic open marine environment to a much reduced oligotrophic condition.

References

Abdel-Kireem, M. R. & Samir, A. M. 1995. Biostratigraphic implications of Maastrichtian-Lower Eocene sequence at the north Gunna section, Farafra Oasis, Western Desert, Egypt. *Marine Micropaleontology* **26**, 329–40.

Alve, E. 1990. Variations in estuarine foraminiferal biofacies with diminishing oxygen conditions in Drammensfjord, S. E. Norway. In *Paleoecology, Biostratigraphy, Paleoceanography, and Taxonomy of Agglutinated Foraminifera* (eds C. Hemleben, D. B. Scott, M. Kaminski & W. Kuhnt), pp. 661–94. Netherlands: Kluwer Academic Publishers.

Alve, E. & Nagy, J. 1986. Estuarine foraminiferal distribution in Sandebukta, a branch of the Oslo Fjord. *Journal of Foraminiferal Research* **16**, 261–84.

Anan, H. S. & Hewaidy, A. A. 1986. Biostratigraphy and distribution of the Paleocene benthonic foraminifera in the Nile Valley Facies in Egypt. Middle East Research Center. *Earth Sciences Series, Ain Shams University* **6**, 1–32.

Awad, G. H. & Ghobrial, M. G. 1965. *Zonal Stratigraphy of the Kharga Oasis*. Geological Survey of Egypt, Cairo, Paper No. 34, 77 pp.

Barthel, K. W. & Herrmann-Degen, W. 1981. Late Cretaceous and Early Tertiary stratigraphy in the Great Sand Sea and its SE Margins (Farafra and Dakhla Oases), SW Desert, Egypt. *Mitteilungen der Bayerischen Staatssammlung für Paläontologie und Historische Geologie* **21**, 141–82.

Berggren, W. A., Kent, D. V., Swisher, C. & Aubry, M. P. 1995. A revised Cenozoic geochronology and chronostratigraphy. In *Geochronology Time Scales and Global Stratigraphic Correlation* (eds W. A. Berggren, D. V. Kent, M. P. Aubry & J. Hardenbol), pp. 129–212. SEPM (Society of Sedimentary Geology), Special Publication no. 54.

Berggren, W.A. & Pearson, P.N. 2005. A revised tropical to subtropical Paleogene planktonic foraminiferal zonation. *Journal of Foraminiferal Research* **35**, 279–98.

Bernhard, J. M. 1987. Foraminiferal biotopes in Explorers Cove, McMurdo Sound, Antarctica. *Journal of Foraminiferal Research* **17**, 286–97.

Cherif, O. H. & Hewaidy, A. A. 1986. The Maastrichtian planktic foraminiferal fauna of the Abu Tartur area, Western Desert, Egypt. *Egyptian Journal Geology* **31**, 217–31.

El-Azabi, M. H. & El-Araby, A. 2000. Depositional cycles, an approach to the sequence stratigraphy of the Dakhla Formation, west Dakhla-Farafra stretch, Western Desert, Egypt. *Journal of African Earth Sciences* **30**, 971–96.

El-Azabi, M. H. & Farouk, S. 2011. High-resolution sequence stratigraphy of the Maastrichtian-Ypresian succession along the eastern scarp face of Kharga Oasis, southern Western Desert, Egypt. *Sedimentology* **58**, 579–617.

El-Dawy, M. H., Obaidalla, N. A., Mahfouz, K. H. & Abdel Wahed, S. A. 2016. Paleocene-Eocene transition at Naqb Assiut, Kharga Oasis, Western Desert, Egypt: Stratigraphical and paleoenvironmental inferences. *Journal of African Earth Sciences* **117**, 207–22.

El deep, W.Z., Faris, M. & Mandur, M.M. 2000. Upper Cretaceous - Lower Paleogene foraminiferal paleoecology of north and southwest Sinai areas, Egypt. *Egyptian Petroleum Journal* **9**, 105–22.

Farouk, S. 2014. Maastrichtian carbon cycle changes and planktonic foraminiferal bioevents at Gebel Matulla, west-central Sinai, Egypt. *Cretaceous Research* **50**, 238–51.

Farouk, S. 2015. Upper Cretaceous sequence stratigraphy of the Galala Plateaux, western side of the Gulf of Suez, Egypt. *Marine and Petroleum Geology* **60**, 136–58.

Farouk, S. 2016. Paleocene stratigraphy in Egypt. *Journal of African Earth Sciences* **113**, 126–52.

Farouk, S. & EL-Sorogy, E. 2015. Danian/Selandian unconformity in the central and southern Western Desert of Egypt. *Journal of African Earth Sciences* **103**, 42–53.

Farouk, S., Marzouk, A. M. & Fayez, A. 2014. The Cretaceous/Paleogene boundary in Jordan. *Journal of Asian Earth Sciences* **94**, 113–25.

Haq, B. U. 2014. Cretaceous eustasy revisited. *Global and Planetary Change* **113**, 44–58.

Haq, B. U. & AL-Qahtani, A. M. 2005. Phanerozoic cycles of sea-level change on the Arabian Platform. *GeoArabia* **10**(2), 127–60.

Haq, B.U., Hardenbol, J. & Vail, P.R. 1987. Chronology of fluctuating sea levels since the Triassic. *Science* **235**, 1156–66.

Hardenbol, J., Thierry, J., Farley, M.B., Jacquin, T., de Graciansky, P. -C. & Vail, P. R. 1998. Mesozoic-Cenozoic sequence chronostratigraphy framework of European basins. In *Sequence Stratigraphy of European Basins* (eds P.-C. de Graciansky, J. Hardenbol, T. Jacquin, & P.R. Vail), pp. 3–14. SEPM (Society for Sedimentary Geology), Special Publication no. 60.

Herrle, J. O., Pross, J., Friedrich, O. & Hemleben, C. 2003*a*. Short-term environmental changes in the Cretaceous Tethyan Ocean: micropaleontological evidence from the Early Albian Oceanic Anoxic Event 1b. *Terra Nova* **15**, 14–9.

Herrle, J. O., Pross, J., Friedrich, O., Köbler, P. & Hemleben, C. 2003*b*. Forcing mechanisms for Mid-Cretaceous black shale formation: evidence from the Upper Aptian and Lower Albian of the Vocontian Basin (SE France). *Palaeogeography, Palaeoclimatology, Palaeoecology* **190**, 399–426.

Hess, S., Nagy, J. & Laursen, G. V. 2014. Benthic foraminifera from the Lower Jurassic transgressive mudstones of the south-western Barents Sea - a possible high-latitude expression of the global Pliensbachian-Toarcian turnover? *Polar Research* **33**, 20206, http://dx.doi.org/10.3402/polar.v33.20206.

Hewaidy, A. A. 1990. Stratigraphy and paleobathymetry of Upper Cretaceous - Lower Tertiary exposures in Beris-Doush area, Kharga Oasis, Western Desert, Egypt. *Qatar University Science Bulletin* **10**, 297–314.

Hewaidy, A. A. & Cherif, O. H. 1984. Contribution to the bathymetric variations of the Late Cretaceous Sea over the Abu Tartur area by using Foraminifera. *Annals of the Geological Survey of Egypt* **15**, 231–41.

Hewaidy, A. A., El-Azabi, M.H. & Farouk, S. 2006. Facies associations and sequence stratigraphy of the Upper Cretaceous-Lower Eocene succession in the Farafra Oasis, Western Desert, Egypt. In *Proceedings of 8th International Conference on Geology of the Arab World (GAW 8)*, Cairo University, Egypt 2, 569–99.

Hewaidy, A. G., Farouk, S., Hatem, A. & Bazeen, Y. 2014. Maastrichtian to Paleocene agglutinated foraminifera from the Dakhla Oasis, Western Desert, Egypt. *Egyptian Journal of Paleontology* **14**, 1–38.

Hewaidy, A. A. & Strougo, A. 2001. Maastrichtian-lower Eocene benthonic foraminiferal distribution and paleoecology of three outcrop sections in Farafra. *Egyptian Journal of Paleontology* **1**, 1–22.

Holbourn, A. E. L., Kuhnt, W. & Erbacher, J. 2001. Benthic foraminifers from Lower Albian black shales (site 1049, ODP Leg 171): Evidence for a non “uniformitarian” record. *Journal of Foraminiferal Research* **31**, 60–74.

Jain, S. & Collins, L. S., 2007. Trends in Caribbean paleoproductivity related to the Neogene closure of the Central American Seaway. *Marine Micropaleontology* **67**, 57–74.

Jain, S., Collins, L. S. & Hayek, L. A.-C. 2007. Relationship of benthic foraminiferal diversity to paleoproductivity in the Neogene of the Caribbean deep-sea. *Palaeogeography, Palaeoclimatology, Palaeoecology* **225**, 223–45.

Jorissen, F. J., De stigter, H. C. & Widmark, J. G. V. 1995. A conceptual model explaining benthic foraminiferal microhabitats. *Marine Micropaleontology* **26**, 3–15.

Kaiho, K. & Hasegawa, T. 1994. End-Cenomanian benthic foraminiferal extinctions and oceanic dysoxic events in the northwestern Pacific Ocean. *Palaeogeography, Palaeoclimatology, Palaeoecology* **111**, 29–43.

Keller, G., Adatte, T., Burns, S. J. & Tantawy, A. A. 2002. High-stress paleoenvironment during the late Maastrichtian to early Paleocene in Central Egypt. *Palaeogeography, Palaeoclimatology, Palaeoecology* **187**, 35–60.

Keller, G., Li, L. & Macleod, N. 1995. The Cretaceous/Tertiary boundary stratotype section at El Kef, Tunisia: how catastrophic was the mass extinction? *Palaeogeography, Palaeoclimatology, Palaeoecology* **119**, 221–54.

King, C. 2013. Paleocene depositional environments and depositional sequences in the Dababiya Quarry Corehole (Egypt). *Stratigraphy* **9**, 347–62.

Le Roy, L. W. 1953. *Biostratigraphy of the Maqfi section, Egypt*. Geological Society of America, Memoir no. 54, 73 pp.

Li, L., Keller, G. & Stinnesbeck, W. 1999. The Late Campanian and Maastrichtian in northwestern Tunisia: Paleoenvironmental inferences from lithology, macrofauna and benthic foraminifara. *Cretaceous Research* **20**, 231–52.

Luger, P. 1985. Stratigraphie der marinen Oberkreide und des Alttertiärs im südlichen Obernil-Becken (SW-Ägypten) unter besonderer Berücksichtigung der Mikropaläontologie, Palökologie und Paläogeographie. *Berliner Geowissenschaftliche Abhandlungen Reihe A* **63**, 1–151.

Luger, P. 1988. Maastrichtian to Paleocene facies evolution and Cretaceous/Tertiary boundary in middle and southern Egypt. *Revista Española de Micropaleontologia, Numero Extraordinario* **1988**, 83–90.

Miller, K. G., Kominz, M. A., Browning, J. V., Wright, J. D., Mountain, G. S., Katz, M. E., Sugarman, P. J., Cramer, B. S., Christie-Blick, N. & Pekar, S. F. 2005. The Phanerozoic record of global sea-level change. *Science* **312**, 1293–8.

Molina, E., Alegret, L., Arenillas, I., Arz, J. A., Gallala, N., Hardenbol, J., Van salis, K., Steurbaut, E., Vandenberghe, N. & Zaghbib-Turki, D. 2006. The Global Boundary Stratotype Section and Point for the base of the Danian Stage (Paleocene, Paleogene, “Tertiary”, Cenozoic) at El Kef, Tunisia - Original definition and revision. *Episodes* **29**, 263–73.

Murray, J. W. 1973. *Distribution and Ecology of Living Benthic Foraminiferids*. London: Heinemann, 288 pp.

Murray, J. W. 2000. When does environmental variability become environmental change? The proxy record of benthic foraminifera. In: *Environmental Micropaleontology* (ed. R.E. Martin)), pp. 7–37. Springer, Topics in Geobiology no. 15.

Murray, J. W. 2006. *Ecology and Applications of Benthic Foraminifera*. New York: Cambridge University Press, 426 pp.

Nagy, J. & Alve, E. 1987. Temporal changes in foraminiferal faunas and impact of pollution in Sandebukta, Oslo Fjord. *Marine Micropaleontology* **12**, 109–28.

Nagy, J., Finstad, E. K., Dypvik, H. & Bremer, M. G. A. 2001. Response of foraminiferal facies to transgressive-regressive cycles in the Callovian of northeast Scotland. *Journal of Foraminiferal Research* **31**, 324–49.

Nagy, J., Hess, S. & Alve, E. 2010. Environmental significance of foraminiferal assemblages dominated by small-sized *Ammodiscus* and *Trochammina* in Triassic and Jurassic strata. *Earth-Science Reviews* **99**, 31–49.

Nagy, J., Hess, S., Dypvik, H. & Bjærke, T. 2011. Marine shelf to paralic biofacies of Upper Triassic to Lower Jurassic deposits in Spitsbergen. *Palaeogeography, Palaeoclimatology, Palaeoecology* **300**, 138–51.

Nagy, J., Løfaldi, m. & Bäckström, S. A. 1988. Aspects of foraminiferal distribution and depositional conditions in Middle Jurassic to Early Cretaceous shales in eastern Spitsbergen. *Abhandlungen der Geologischen Bundesanstalt* **30**, 297–300.

Nagy, J., Pilskog, B. & Wilhelmsen, R. 1990. Facies controlled distribution of foraminifera in the Jurassic North Sea Basin. In *Paleoecology, Biostratigraphy, Paleoceanography and Taxonomy of Agglutinated Foraminifera* (eds C. Hemleben, M. A. Kaminski, W. Kuhnt, & D. B. Scott), pp. 621–57. Dordrecht, The Netherlands: Kluwer Academic Press.

Orabi, H. O. & Khalil, H. M. 2014. Calcareous benthonic foraminifera across the Cretaceous/Paleocene transition of Gebel Um El-Ghanayem, Kharga Oasis, Egypt. *Journal of African Earth Sciences* **96**, 110–21.

Said, R. 1962. *The Geology of Egypt*. Amsterdam: Elsevier, 377 pp.

Said, R. & Kerdany, M. T. 1961. The geology and micropaleontology of Farafra Oasis. *Micropaleontology* **7**(3), 317–36.

Samir, A. M. 1995. Paleoenvironmental significance of the Upper Cretaceous-Lower Tertiary foraminifera of the North Gunna section, Farafra Oasis, Western Desert, Egypt. Proceedings. *Koninklijke Nederlandsch Akademie van Wetenschappen* **98**, 109–26.

Schnack, K. 2000. Biostratigraphie und fazielle Entwicklung in der Oberkreide und im Alttertiär im

Bereich der Kharga Schwelle, Westliche Wüste, SW Ägypten. *Berichte aus dem Fachbereich Geowissenschaften der Universität Bremen* **151**, 1–142.

Sebei, K., Inoubli, M. H., Boussiga, H., Tlig, S., Alouani, R. & Boujamaoui, M. 2007. Seismic stratigraphy, tectonics and depositional history in the Halk el Menzel region, NE Tunisia. *Journal of African Earth Sciences* **47**, 9–29.

Smart, C. W. 1998. Diversity patterns of Miocene benthic foraminifera in the Somali Basin, northwestern Indian Ocean. *Micropaleontology* **44**, 256–64.

Speijer, R. P. 1994. Extinction and recovery patterns in benthonic foraminiferal paleocommunities across the Cretaceous/Paleogene and Paleocene/Eocene boundaries. *Mededlingen Van de Faculteit Aurdwetenschappen Universiteit Utrecht* 124–91.

Speijer, R. P., Schmitz, B., Aubry, M. -P. & Charisi, S. D. 1996. The latest Paleocene benthic extinction event: Punctuated turnover in outer neritic foraminiferal faunas from Gebel Aweina, Egypt. *Israel Journal of Earth Sciences* **44**, 207–22.

Speijer, R. P. & Van der zwaan, G. J. 1996. Extinction and survivorship of southern Tethyan benthic foraminifera across the Cretaceous/Paleogene boundary. In *Biotic Recovery from Mass Extinction Events* (ed. M.B. Hart), pp. 343–72. Geological Society of London, Special Publication no. 102.

Tantawy, A. A., Keller, G., Adatte, T., Stinnesbeck, W., Kassab, A. & Schulte, P. 2001. Maastrichtian to Paleocene depositional environment of the Dakhla Formation, Western Desert, Egypt: Sedimentology, mineralogy, and integrated micro- and macrofossil biostratigraphies. *Cretaceous Research* **22**, 795–827.

Van Der Zwaan, G. J., Duijnstee, I. A. P., Den dulk, M., Ernst, S. R., Jannink, N. T. & Kouwenhoven, T. J. 1999. Benthic foraminifers: proxies or problems? A review of paleocological concepts. *Earth Science Reviews* **46**, 213–36.

Voigt, S., Gale, A. S., Jung, C. & Jenkyns, H. C. 2012. Global correlation of Upper Campanian-Maastrichtian successions using carbon-isotope stratigraphy: development of a new Maastrichtian timescale. *Newsletters on Stratigraphy* **45**, 25–53.